Local Optical Spectroscopy in Quantum Confined Systems: A Theoretical Description

Local Optical Spectroscopy in Quantum Confined Systems: A Theoretical Description

Oskar Mauritz, Guido Goldoni, Fausto Rossi, and Elisa Molinari
Istituto Nazionale per la Fisica della Materia (INFM), and Dipartimento di Fisica, Università di Modena, Via Campi 213A, I-41100 Modena, Italy
(Received 17 July 1998)

A theoretical description of local absorption is proposed in order to investigate spectral variations on a length scale comparable with the extension of the relevant quantum states. A general formulation, including Coulomb correlation, is derived within the density-matrix formalism and applied to the prototypical case of coupled quantum wires. The results show that excitonic effects may have a crucial impact on the local absorption, with implications for the spatial resolution and the interpretation of near-field optical spectra. [S0031-9007(98)08294-5]

PACS numbers: 78.66.Fd, 71.35.–y, 73.20.Dx, 78.40.Fy

The achievement of very high spatial resolutions in optical spectroscopies of molecules and solids is among the important experimental advancements of recent years. While in conventional optical experiments the light field is essentially constant in amplitude and phase over the spatial extension of the relevant quantum mechanical states, microprobe techniques make use of highly inhomogeneous light fields. In the case of low-dimensional semiconductors, diffraction-limited confocal microscopy has allowed the study of individual nanostructures and their geometrical fluctuations [1]. With near-field scanning optical microscopy (NSOM), the spatial resolution is reduced below the diffraction limit and approaches the scale of quantum confinement [2]: optical spectroscopy thus becomes a powerful probe of the spatial distribution of quantum states.

In analogy with ultrafast time-resolved spectroscopies [3] that have shown the importance of phase coherence in the quantum-mechanical time evolution of photoexcited carriers [4], it may be expected that spatial interference of quantum states plays a dominant role when variations of the electromagnetic (EM) field occur on an ultrashort length scale. On the theoretical side, however, not much work has been done to investigate the response under these conditions. Most work has focused on the near-field distribution of the EM field [5] and its interaction with arrays of pointlike particles [6], and only recently the effect of an inhomogeneous EM field on single-particle transitions has been modeled for a semiconductor quantum dot [7].

In this Letter we propose a theoretical formulation, not limited to low photoexcitation densities, based on a fully microscopic description of electronic quantum states and their Coulomb correlation. We show that the nonlocal character of light-matter interaction must be taken into account, and demonstrate that for any given shape of the EM-field distribution a proper definition of local absorption can still be introduced. By applying this scheme to the prototypical case of a coupled quantum-wire structure, we prove that, when very high resolution is achieved, nonlocal and Coulomb-correlation effects dominate the local spectra which, therefore, cannot be simply interpreted as a map of the single-particle wave functions.

The macroscopic polarization $\mathbf{P}(\mathbf{r}, \omega)$ induced by an electromagnetic field $\mathbf{E}(\mathbf{r}, \omega)$ is in general given by

$$\mathbf{P}(\mathbf{r}, \omega) = \int \boldsymbol{\chi}(\mathbf{r}, \mathbf{r}', \omega) \cdot \mathbf{E}(\mathbf{r}', \omega)\, d\mathbf{r}', \qquad (1)$$

where $\boldsymbol{\chi}(\mathbf{r}, \mathbf{r}', \omega)$ is the nonlocal susceptibility tensor. It can be regarded as the Fourier transform of the local polarization, whose microscopic expression is given by

$$\mathbf{P}(\mathbf{r}, t) = q\langle \hat{\boldsymbol{\Psi}}^{\dagger}(\mathbf{r}, t)\mathbf{r}\hat{\boldsymbol{\Psi}}(\mathbf{r}, t)\rangle, \qquad (2)$$

where q is the electronic charge, $\langle \cdots \rangle$ denotes a proper ensemble average, and the field operator $\hat{\boldsymbol{\Psi}}(\mathbf{r}, t)$ in the Heisenberg picture describes the microscopic evolution of the carrier system. Within the usual electron/hole picture, the optical (i.e., interband) contribution to $\mathbf{P}(\mathbf{r}, t)$ can be expressed in terms of the nondiagonal elements of the single-particle density matrix $p_{eh} = \langle \hat{d}_h \hat{c}_e \rangle$ ($\hat{d}_h$ and $\hat{c}_e$ being the destruction operators for a hole in state h and an electron in state e) according to

$$\mathbf{P}(\mathbf{r}, t) = q \sum_{eh} [\, p_{eh}(t)\Psi_e(\mathbf{r})\mathbf{r}\Psi_h(\mathbf{r}) + \text{c.c.}]. \qquad (3)$$

Here, e and h are appropriate sets of quantum numbers which label the free-carrier wave functions $\Psi_{e/h}$ involved in the optical transition. The time evolution of the single-particle density matrix is described by the semiconductor Bloch equations [8], which for the nondiagonal elements (interband polarizations) read [9]

$$\frac{\partial p_{eh}}{\partial t} = \frac{1}{i\hbar}(\mathcal{E}_e + \mathcal{E}_h)p_{eh} + \frac{1}{i\hbar}\mathcal{U}_{eh}(1 - f_e - f_h) + \left.\frac{\partial p_{eh}}{\partial t}\right|_{\text{coll}}, \qquad (4)$$

where $\mathcal{U}_{eh}$ and $\mathcal{E}_{e/h}$ are, respectively, the EM-field and single-particle energies renormalized by the Coulomb interaction. The last (collision) term in Eq. (4) accounts for incoherent (i.e., scattering and diffusion) processes [10]. Stationary solutions of this equation can be found by assuming equilibrium distribution functions f_e, f_h; in this

case Eq. (4) can be transformed into an eigenvalue equation whose λth solution provides the complex energy eigenvalue $\hbar\omega^\lambda = \epsilon^\lambda - i\Gamma^\lambda$ and eigenvector p^λ_{eh}.

By inserting the stationary solution $p_{eh}(t) = p^\lambda_{eh} e^{-i\omega^\lambda t}$ of Eq. (4) into Eq. (3) and Fourier transforming, it is possible to express the polarization $\mathbf{P}(\mathbf{r}, \omega)$ in the form of Eq. (1), from which a microscopic expression for $\boldsymbol{\chi}$ can be identified. In particular, for semiconductor structures described within the usual envelope-function formalism with isotropic electron and hole bulk dispersions, the susceptibility tensor $\boldsymbol{\chi}$ becomes diagonal, with identical elements given by

$$\chi(\mathbf{r}, \mathbf{r}', \omega) = |M_b|^2 \sum_{\lambda, eh, e'h'} p^\lambda_{eh} p^{\lambda *}_{e'h'} (1 - f_{e'} - f_{h'}) \times \frac{\psi_e(\mathbf{r}) \psi_h(\mathbf{r}) \psi^*_{e'}(\mathbf{r}') \psi^*_{h'}(\mathbf{r}')}{\epsilon^\lambda - \hbar\omega - i\Gamma^\lambda}. \quad (5)$$

Here, $\psi_{e/h}(\mathbf{r})$ are single-particle electron/hole envelope functions and M_b is the bulk optical matrix element.

In the usual definition of the absorption coefficient within the dipole approximation, the nonlocality of χ is neglected. When nonlocality is taken into account, it is no longer possible to define an absorption coefficient that locally relates the absorbed power density with the light intensity. However, considering a light field with a given profile ξ centered around the beam position $\mathbf{R}$, $E(\mathbf{r}, \omega) = E(\omega)\xi(\mathbf{r} - \mathbf{R})$, we may define a local absorption that is a function of the beam position, and relates the *total* absorbed power to the power of a *local* excitation (illumination mode),

$$\alpha_\xi(\mathbf{R}, \omega) \propto \int \mathrm{Im}[\chi(\mathbf{r}, \mathbf{r}', \omega)] \times \xi(\mathbf{r} - \mathbf{R}) \xi(\mathbf{r}' - \mathbf{R})\, d\mathbf{r}\, d\mathbf{r}'. \quad (6)$$

This expression is in principle not limited to low-photoexcitation intensities; together with Eq. (5) it provides a general description of linear as well as nonlinear local response, i.e., from excitonic absorption to the gain regime.

In the linear-response regime $1 - f_e - f_h \simeq 1$ and the quantity $\Psi^\lambda(\mathbf{r_e}, \mathbf{r_h}) = \sum_{eh} p^\lambda_{eh} \psi_e(\mathbf{r_e}) \psi_h(\mathbf{r_h})$ can be identified with the exciton wave function; in this case the nonlocal susceptibility (5) reduces to the result of linear-response theory as given, e.g., in [11]. In this regime the contribution of the λth excitonic state to the local spectrum is

$$\alpha_\xi(\mathbf{R}, \omega^\lambda) \propto \left| \int \Psi^\lambda(\mathbf{r}, \mathbf{r}) \xi(\mathbf{r} - \mathbf{R})\, d\mathbf{r} \right|^2. \quad (7)$$

The above formulation is valid for semiconductors of arbitrary dimensionality. To illustrate the effects of nonlocality and Coulomb correlation on the local absorption spectrum, we now consider quasi-one-dimensional (quasi-1D) nanostructures (quantum wires), subject to a local EM excitation propagating parallel to the free axis of the structure, z. For simplicity, we describe the narrow light beam by a Gaussian EM-field profile, $\xi(\mathbf{r}) = \exp[-(x^2 + y^2)/2\sigma^2]$ [12]. For a quantum wire the single-particle electron/hole wave functions appearing in (5) can be written as $\psi_e(\mathbf{r}) = \phi_{\nu_e}(x, y) e^{ik^e_z z}$, $\psi_h(\mathbf{r}) = \phi_{\nu_h}(x, y) e^{ik^h_z z}$ where $\nu_{e/h}$ are subband indices and $k^{e/h}_z$ are wave vectors along the free axis.

To discuss the 1D case it is convenient to take advantage of the translational invariance along z and define

$$\Phi^\lambda(x, y) \equiv \int \Psi^\lambda(\mathbf{r}, \mathbf{r})\, dz \propto \sum_{\nu_e \nu_h k_z} p^\lambda_{\nu_e k_z \nu_h - k_z} \phi_{\nu_e}(x, y) \phi_{\nu_h}(x, y). \quad (8)$$

We shall refer to $\Phi^\lambda(x, y)$ as the *effective* exciton wave function. $\Phi^\lambda(x, y)$ enters Eq. (7) and, convoluted with the spatial distribution of the EM field, ξ, yields the contribution of the λth excitonic state to the local absorption $\alpha_\xi(X, Y, \omega)$; note that only Fourier components of the polarization with $k^e_z = -k^h_z$ contribute to the absorption.

The effects of spatial coherence of quantum states are understood most easily in the linear regime on the basis of Eq. (7). For a spatially homogeneous EM field, the absorption spectrum probes the average of Φ^λ over the whole space (global spectrum). In the opposite limit of an infinitely narrow probe beam, $\alpha(X, Y, \omega^\lambda)$ maps $|\Phi^\lambda(X, Y)|^2$; the local absorption is nonzero at any point where the effective wave function of an exciton gives a finite contribution. It is therefore clear that "forbidden" excitonic transitions, not present in the global spectrum, may appear in the local one. In the intermediate regime of a narrow but finite probe, it is possible that a cancellation of the contributions from $\Phi^\lambda(x, y)$ takes place between different points in space leading to a nontrivial localization of the absorption. The result will then be quite sensitive to the extension of the light beam.

As a prototype system showing nonlocal effects we consider two coupled GaAs/AlAs T-shaped wires [13]. To obtain spatially separated transitions we consider an asymmetric structure (Fig. 1); the barrier width is chosen to allow Coulomb coupling between the wires [14]. For both electrons and holes, the single-particle ground state $(E1, H1)$ is localized in the widest wire (right wire, RW) and the second bound state $(E2, H2)$ in the left wire (LW) [15]. The effective exciton wave functions Φ^λ are shown in Fig. 1 for the ground state exciton and for one of the excited states. They are found to differ significantly from the single-particle wave functions (not shown here); this is true in general for coupled nanostructures. The ground state exciton mainly involves single-particle contributions from the first electron and first hole subband ($E1$-$H1$), and has no nodes; hence, no cancellation is possible, and its contribution to the local spectrum is expected to be finite for any extension of the probe beam. On the other hand, the effective exciton wave function for the higher state

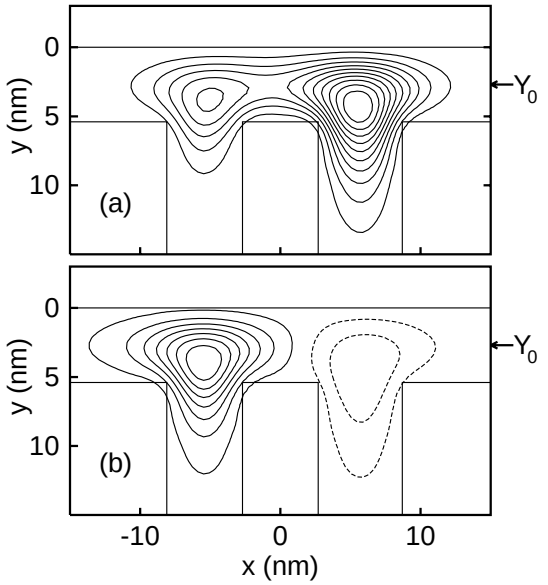

FIG. 1. Effective exciton wave functions $\Phi^{\lambda}(x, y)$ for two coupled T-shaped GaAs/AlAs quantum wires, formed at the intersections between two vertical quantum wells (5.4 and 6.0 nm wide, with a 5.4 nm barrier) and a horizontal quantum well (5.4 nm wide). Only the dominant (real) part of the complex wave function is shown for (a) the ground state exciton, and (b) one of the excited states giving rise to the shoulder labeled D in Figs. 2 and 3. Dashed contours correspond to negative values. Note the two distinct regions with different sign, giving rise to cancellation effects for sufficiently large values of σ.

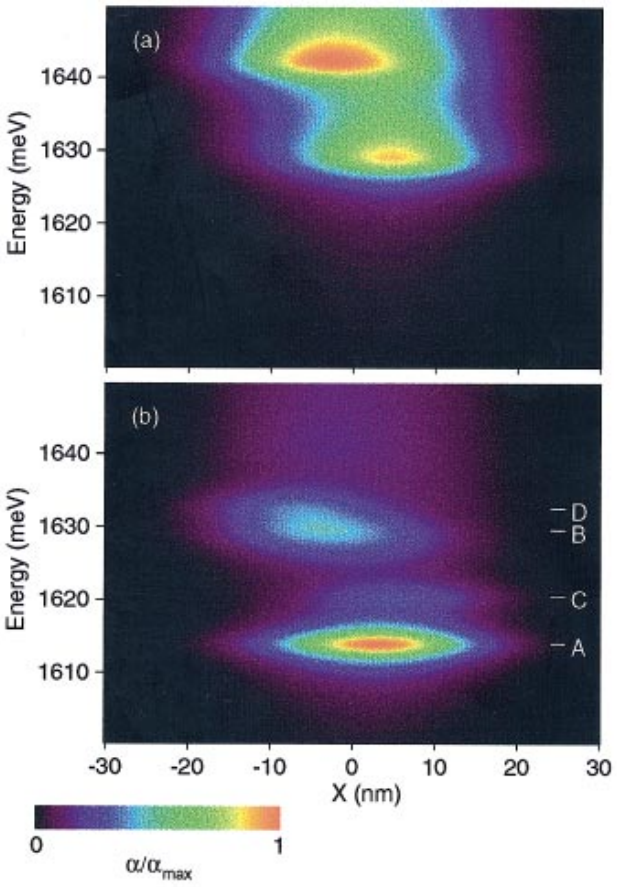

FIG. 2(color). Local absorption $\alpha(X, Y, \hbar\omega)$ as a function of photon energy and beam position. The beam coordinate X varies across the wires parallel to the x direction, with $Y = Y_0$ fixed at the center of the horizontal quantum well (see Fig. 1); $\sigma = 10$ nm. The absorption is normalized so that the maximum absorption, $\alpha_{\max}$, is the same in both maps. (a) Spectrum calculated in the single-particle approximation; (b) full calculation, with the electron-hole Coulomb correlation taken into account. The labels A, B, C, D identify the main structures discussed in the text.

has areas with different signs; therefore its convolution with ξ may produce cancellations, whose results depend strongly on the characteristic spatial extension of the beam, σ. Of course, the phase of the relevant quantum states is determined by electron-hole correlations on the scale of the exciton Bohr radius; therefore, to emphasize these effects, in the following we show calculations for a beam with $\sigma = 10$ nm (close to the Bohr radius a_0 in GaAs). Note that NSOM experiments on semiconductors are currently still limited to higher values of σ; calculations performed for $\sigma \gg a_0$ confirm that these effects become negligible, so that a local description is sufficient.

Figure 2 shows the local absorption $\alpha(X, Y, \hbar\omega)$ in the linear regime as a function of photon energy and beam position. $Y = Y_0$ is fixed at the center of the horizontal quantum well (see Fig. 1), while the X coordinate varies across the structure. As a reference we first discuss results in the absence of electron-hole interaction [Fig. 2(a)]: the spectrum is essentially composed of two structures, both with the typical inverse-square root high energy tail ensuing from the 1D free-particle density of states. The signal from the $E1$-$H1$ transition is spatially located on the RW while a second peak, located on the LW, stems from the $E2$-$H2$ transition; in this uncorrelated case the influence of spatially indirect transitions ($E1$-$H2$, $E2$-$H1$) is negligible. The correlated carrier spectrum [Fig. 2(b)] is very different. As expected, the spectrum is dominated by excitonic peaks at lower energies (the ground state binding energy is 14 meV [16]), and the corresponding continuum is strongly suppressed by the electron-hole interaction [9]. The two main peaks (A and B, at $\approx$1614 and 1629 meV, respectively) still have their largest contributions in the RW and LW, respectively; however, two weaker structures C and D appear (at $\approx$1620 and $\approx$1633 meV, respectively), which are more strongly localized in either wire and have no equivalent in the uncorrelated spectrum.

We analyze the origin and spatial localization of these structures with the help of Fig. 3, which shows the local spectra with the beam centered on the RW or the LW, as well as the global spectrum [17]. The most intense peak (A) is the ground state exciton ($E1$-$H1$); it has the strongest contribution from the RW, but a significant intensity is found also in the LW, consistently with the

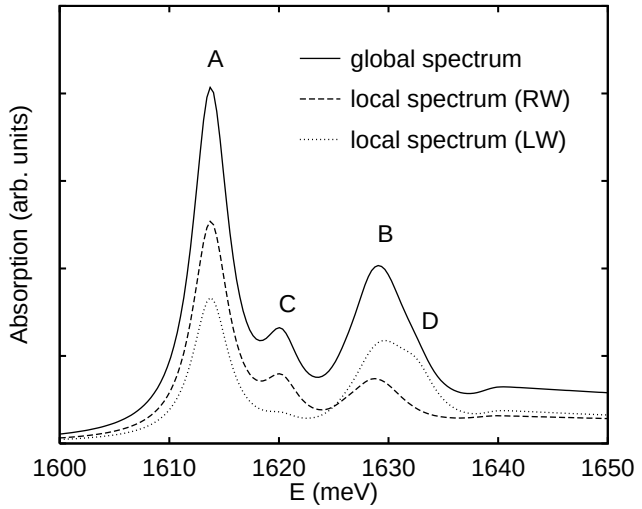

FIG. 3. Global (solid line) and local absorption spectra (including electron-hole correlation), calculated with the beam centered on the right wire (dashed line) and on the left wire (dotted line); $\sigma = 10$ nm. The labels A, B, C, D identify the main structures discussed in the text.

spatial extension of its effective wave function [Fig. 1(a)]. Peak C also originates from the RW where a second bound exciton is introduced in the presence of Coulomb coupling with the LW; indeed, this structure is not present when the wires are far apart. Peak B stems from several exciton states, with a major component in the $E2$-$H2$ transition on the LW. The shoulder D (mostly a $E2$-$H1$ transition) is very intense in the local spectrum centered on the LW, completely absent when the beam is centered on the RW, and obviously very reduced in the global spectrum. A detailed analysis shows that the strong localization of D comes from the interference between positive and negative regions of the effective exciton wave function [Fig. 1(b)], whose cancellation depends on the position of the beam.

Similar calculations for other types of coupled nanostructures confirm that these phenomena are general, and especially significant when they are investigated with spatial resolution of the order of the Bohr radius. At such resolutions, the breaking of selection rules that hold in integrated spectra might then give insight into Coulomb correlation and coherence phenomena.

In summary, we have presented a general formulation of local optical absorption, holding for any given profile of the light beam even when its width becomes comparable to the exciton Bohr radius in the semiconductor. The key ingredient is the effective exciton wave function, whose interference effects have a very different influence on local and global spectra. As the spatial resolution of near-field optical experiments increases, these effects are expected to become important in the interpretation of local spectra.

This work was supported in part by the MURST-40% program "Physics of Nanostructures" and by the EC Commission through the TMR Network "Ultrafast Quantum Optoelectronics."

[1] See, e.g., A. Zrenner *et al.*, Phys. Rev. Lett. **72**, 3642 (1994); D. Gammon *et al.*, Phys. Rev. Lett. **76**, 3005 (1996); J. Hasen *et al.*, Nature (London) **390**, 54 (1997).
[2] E. Betzig *et al.*, Science **251**, 1468 (1993); H. F. Hess *et al.*, Science **264**, 1740 (1994).
[3] J. Shah, *Ultrafast Spectroscopy of Semiconductors and Semiconductor Nanostructures* (Springer, Berlin, 1996).
[4] A. P. Heberle, J. J. Baumberg, and K. Kohler, Phys. Rev. Lett. **75**, 2598 (1995).
[5] R. Chang *et al.*, J. Appl. Phys. **81**, 3369 (1997).
[6] B. Hanewinkel *et al.*, Phys. Rev. B **55**, 13 715 (1997).
[7] G. W. Bryant, Appl. Phys. Lett. **72**, 768 (1998).
[8] T. Kuhn, in *Theory of Transport Properties of Semiconductor Nanostructures*, edited by E. Schöll (Chapman & Hall, London, 1998), p. 173.
[9] F. Rossi and E. Molinari, Phys. Rev. Lett. **76**, 3642 (1996); Phys. Rev. B **53**, 16 462 (1996).
[10] For a discussion of these effects at different temperatures in quantum wires see A. Richter *et al.*, Phys. Rev. Lett. **79**, 2145 (1997). In our calculations we treat the collision term within the relaxation time approximation.
[11] A. D'Andrea and R. Del. Sole, Phys. Rev. B **25**, 3714 (1982).
[12] The actual profile of the EM field generated by a NSOM tip is more complex, and a research topic in itself [5–7]. However, our simple choice for ξ is sufficient to highlight the effects of nonlocality. An arbitrary field distribution can be included in our treatment through Eq. (6), while Eq. (5) is independent of the external field.
[13] NSOM studies of T-shaped wires exist in the literature, but have so far focused on characterization of the structures: R. D. Grober *et al.*, Appl. Phys. Lett. **64**, 1421 (1994); T. D. Harris *et al.*, Appl. Phys. Lett. **68**, 988 (1996).
[14] Calculations are performed according to Refs. [9,16]; the single-particle states are solutions of the Schrödinger-like equation for envelope functions. The full three-dimensional nature of the Coulomb interaction is retained by expanding the excitonic state on the basis of single-particle transitions.
[15] In the present calculations valence band mixing is neglected [G. Goldoni *et al.*, Phys. Rev. B **55**, 7110 (1997)]. We use homogeneous and isotropic effective masses $m^e = 0.067m_0$ and $m^h = 0.34m_0$; the GaAs/AlAs band offsets are $V^e = 1.033$ eV and $V^h = 0.558$ eV.
[16] F. Rossi, G. Goldoni, and E. Molinari, Phys. Rev. Lett. **78**, 3527 (1997).
[17] For clarity, in the present calculations we have neglected higher-energy states from the wider QW. We have checked that these do not affect the local spectra in Fig. 3, but would contribute only to the high-energy part of the global spectrum in the same figure.